 Related Commentary, page 1082

Requirement for Ca^{2+}/calmodulin–dependent kinase II in the transition from pressure overload–induced cardiac hypertrophy to heart failure in mice

Haiyun Ling,[1] Tong Zhang,[1] Laetitia Pereira,[2] Christopher Kable Means,[1] Hongqiang Cheng,[3] Yusu Gu,[3] Nancy D. Dalton,[3] Kirk L. Peterson,[3] Ju Chen,[3] Donald Bers,[2] and Joan Heller Brown[1]

[1]Department of Pharmacology, UCSD, La Jolla, California, USA. [2]Department of Pharmacology, UCD, Davis, California, USA. [3]Department of Medicine, UCSD, La Jolla, California, USA.

Ca^{2+}/calmodulin–dependent kinase II (CaMKII) has been implicated in cardiac hypertrophy and heart failure. We generated mice in which the predominant cardiac isoform, CaMKIIδ, was genetically deleted (KO mice), and found that these mice showed no gross baseline changes in ventricular structure or function. In WT and KO mice, transverse aortic constriction (TAC) induced comparable increases in relative heart weight, cell size, HDAC5 phosphorylation, and hypertrophic gene expression. Strikingly, while KO mice showed preserved hypertrophy after 6-week TAC, CaMKIIδ deficiency significantly ameliorated phenotypic changes associated with the transition to heart failure, such as chamber dilation, ventricular dysfunction, lung edema, cardiac fibrosis, and apoptosis. The ratio of IP_3R2 to ryanodine receptor 2 (RyR2) and the fraction of RyR2 phosphorylated at the CaMKII site increased significantly during development of heart failure in WT mice, but not KO mice, and this was associated with enhanced Ca^{2+} spark frequency only in WT mice. We suggest that CaMKIIδ contributes to cardiac decompensation by enhancing RyR2-mediated sarcoplasmic reticulum Ca^{2+} leak and that attenuating CaMKIIδ activation can limit the progression to heart failure.

Introduction

It is well accepted that altered intracellular Ca^{2+} handling plays an important role in the pathogenesis of heart failure and that changes in Ca^{2+} cycling can precede development of cardiac dysfunction. The calcium-activated signaling molecule Ca^{2+}/calmodulin–dependent kinase II (CaMKII) phosphorylates and regulates a number of key proteins involved in intracellular Ca^{2+} homeostasis, including phospholamban (PLB), ryanodine receptors (RyRs), and the L-type channel (1–10). CaMKII has been associated with the development of heart failure through a variety of observations. First, upregulation of CaMKII expression and activity have been reported to be a general feature of heart failure in humans and in animal models (11–14). In addition, our previous work has shown that cardiac-specific overexpression of CaMKIIδ induces a hypertrophic phenotype that, for the $CaMKII\delta_C$ splice variant, rapidly transitions to dilated cardiomyopathy with ventricular dysfunction, loss of intracellular Ca^{2+} homeostasis, and premature death (15–18). Further evidence linking CaMKII and heart failure comes from studies demonstrating that CaMKII inhibition by either pharmacological or genetic approaches reverses heart failure–associated changes (i.e., arrhythmias, hypertrophy, and dysfunction) in animal models of structural heart disease (19–21).

More compelling evidence for an in vivo function of CaMKII in cardiac remodeling would derive from studies using mice lacking the CaMKII gene. CaMKII is encoded by 4 genes (*Camk2a*, *Camk2b*, *Camk2d*, and *Camk2g*), of which the δ and γ isoforms are expressed in heart (22), with δ as the predominant isoform (23–26). Accordingly, we set out to generate mice in which the CaMKIIδ isoform was genetically deleted. Our results revealed that germline ablation of CaMKIIδ had no detectable baseline effects on cardiac structure or function and that CaMKIIδ deletion did not substantially affect the development of cardiac hypertrophy after pressure overload. Remarkably, however, the absence of CaMKIIδ significantly attenuated the development of pressure overload–induced heart failure and improved survival, concomitant with decreases in cardiac dysfunction, cardiomyocyte apoptosis, and fibrosis. We suggest that CaMKIIδ-mediated changes in Ca^{2+} handling, including phosphorylation of RyR2 at the CaMKII site and increased diastolic sarcoplasmic reticulum (SR) Ca^{2+} leak, underlie the decompensation from cardiac hypertrophy to heart failure.

Results

Characterization of conventional CaMKIIδ-deficient mice. Homozygous CaMKIIδ-null mice, referred to herein as KO mice, were generated from heterozygous CaMKIIδ mice and born at normal Mendelian ratios. We identified these mice by Southern blotting (Figure 1B), PCR analysis of genomic DNA isolated from mouse tails (Figure 1C), and the absence of CaMKIIδ protein on Western blot-

Conflict of interest: The authors have declared that no conflict of interest exists.

Nonstandard abbreviations used: CaMK, Ca^{2+}/calmodulin–dependent kinase; CaSpF, Ca^{2+} spark frequency; -d, in diastole; FS, fractional shortening; HDAC, class II histone deacetylase; HW, heart weight; IP_3R2, type 2 inositol 1,4,5 trisphosphate receptor; IVS, interventricular septal thickness; LVID, LV internal diameter; LVPW, LV posterior wall thickness; LW, lung weight; MEF2, myocyte enhancer factor 2; PLB, phospholamban; RyR, ryanodine receptor; -s, in systole; SERCA2, sarcoplasmic or endoplasmic reticulum calcium ATPase2; SR, sarcoplasmic reticulum; TAC, transverse aortic constriction; TL, tibial length.

Citation for this article: *J. Clin. Invest.* **119**:1230–1240 (2009). doi:10.1172/JCI38022.

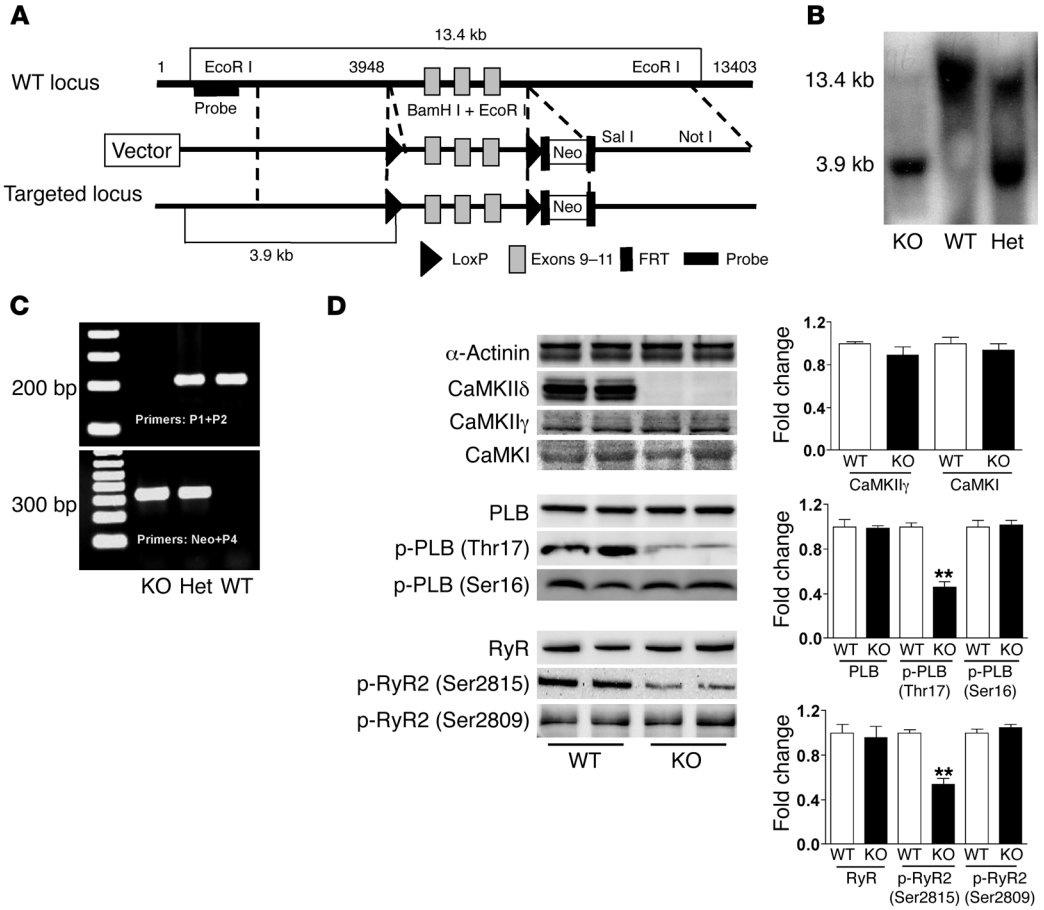

Figure 1

Generation and characterization of mice with CaMKIIδ deletion. (**A**) Restriction map of the genomic structure of the *Camk2d* gene, the targeting construct, and the mutated locus after recombination. The targeting construct was generated by flanking exons 9–11 of *Camk2d* with 2 loxP sites and flanking the Neo cassette by Flp recombinase target (FRT) sites. (**B**) Genotyping of CaMKIIδ-deficient mice by Southern blot analysis with the probe shown in **A**. Genomic DNA was isolated from the tails of a WT, a KO, and a heterozygous (Het) mouse. The 13.4- and 3.9-kb bands represent WT and mutant alleles, respectively. (**C**) Genotyping of KO mice by PCR analysis using mouse tail DNA and specific primers for the WT (P1+P2) and mutant (Neo+P4) alleles. (**D**) Analysis of protein expression and phosphorylation in WT and CaMKIIδ-deficient mice. LV homogenates were subjected to Western blotting. Quantitative analysis of the expression and phosphorylation of the proteins is shown at right. Data are mean ± SEM of 4–7 determinations. $^{**}P < 0.01$ versus WT.

ting (Figure 1D). The KO mice showed no increase in mortality or apparent physical abnormalities during follow-up for over 10 months. In KO mice, there were no changes in the basal expression or phosphorylation level of 2 CaMKII substrates, PLB and RyR, at their PKA phosphorylation sites (PLB at Ser16 and RyR2 at Ser2809). However, the phosphorylation of PLB and RyR2 at CaMKII sites (PLB at Thr17 and RyR2 at Ser2815) substantially decreased (Figure 1D), which indicates that CaMKIIδ plays a critical role in basal PLB and RyR2 phosphorylation. We also examined the possibility that systemic deletion of CaMKIIδ would lead to compensatory changes in other CaMK isoforms. Western blot analysis revealed no increase in expression of either CaMKIIγ or CaMKI in the KO mice (Figure 1D).

Deletion of CaMKIIδ did not measurably affect ventricular chamber dimension or wall thickness, as assessed by echocardiography, in mice at 2 or 10 months of age (Table 1). The contractile and relaxant responses to dobutamine stimulation were also assessed by hemodynamic measurement in 3-month-old KO and WT littermates. There was no measurable difference in the functional responses to dobutamine between WT and KO mice (Table 2). Thus we conclude that germline ablation of CaMKIIδ has no evident baseline effects on ventricular structure or function.

CaMKIIδ deletion does not inhibit cardiac hypertrophy induced by 2-week transverse aortic constriction. Based on the cardiac hypertrophic and heart failure phenotypes previously developed in transgenic mice overexpressing CaMKIIδ (15, 16), we expected to observe a reduced hypertrophic response in KO mice subjected to pressure overload induced by transverse aortic constriction (TAC). However, gravimetric analysis showed that ratios of heart weight (HW) to BW and HW to tibial length (TL) were comparably increased in WT and KO mice subjected to 2-week TAC, with similar pressure gradients (WT, 125 ± 11 mmHg; KO, 101 ± 19 mmHg; Figure 2A). There were also similar increases in myocyte cross-sectional area (Figure 2A), echocardiographic endpoints (Table 3), and hypertrophic gene expression (Figure 2B). Recently, the Olson laboratory reported that CaMKIIδ deletion blocks pathological cardiac

Table 1
Basal echocardiographic parameters in mice with CaMKIIδ deletion and their WT littermates at 2 and 10 months of age

Parameter	2 mo		10 mo	
	WT	KO	WT	KO
HR (bpm)	578 ± 57	563 ± 60	603 ± 71	588 ± 54
IVSd (mm)	0.60 ± 0.04	0.59 ± 0.03	0.68 ± 0.14	0.72 ± 0.16
IVSs (mm)	1.00 ± 0.08	1.04 ± 0.21	1.17 ± 0.16	1.22 ± 0.17
LVPWd (mm)	0.60 ± 0.04	0.60 ± 0.04	0.68 ± 0.14	0.71 ± 0.15
LVPWs (mm)	1.13 ± 0.09	1.10 ± 0.07	1.24 ± 0.20	1.30 ± 0.13
LVIDd (mm)	3.52 ± 0.34	3.40 ± 0.35	3.49 ± 0.52	3.60 ± 0.46
LVIDs (mm)	1.99 ± 0.30	1.98 ± 0.36	1.89 ± 0.53	2.00 ± 0.43
FS (%)	43.6 ± 4.9	42.0 ± 8.4	46.5 ± 8.4	45.0 ± 5.7

Data are mean ± SD from 10–26 mice. HR, heart rate.

hypertrophy induced by pressure overload (27). However, in our genetically altered mouse model, deletion of CaMKIIδ clearly did not inhibit the hypertrophic response to pressure overload.

Class II histone deacetylases (HDACs) such as HDAC4 and HDAC5 have been demonstrated to be substrates for CaMKII and PKD (28–30) and act as repressors of myocyte enhancer factor 2 (MEF2). Phosphorylation of these HDACs enables MEF2-mediated transactivation of hypertrophic marker genes. While 2-week TAC did not increase HDAC4 phosphorylation (data not shown), it led to significant and comparable increases in Ser498-phosphorylated HDAC5 in both KO mice and WT littermates (Figure 2C).

Upregulation of CaMKIIγ and PKD expression and activation in cardiac hypertrophy. While CaMKIIδ has previously been shown to predominate in the heart, CaMKIIγ is also present (22, 31, 32). Pressure overload was previously shown to increase expression of CaMKIIγ as well as CaMKIIδ (16, 33). We examined the effect of 2-week TAC on the expression of CaMKIIδ and CaMKIIγ in WT and KO mice and found that both isoforms were upregulated in WT mice (Figure 3A). A similar increase in CaMKIIγ was also seen in the banded KO mice. Studies using a phospho-CaMKII antibody to determine the amount of active CaMKII revealed that phospho-CaMKII levels were increased to a similar extent by TAC in both WT and KO mice (Figure 3A). Because the phospho-CaMKII antibody does not distinguish the CaMKII isoforms, we suggest that the increase in phospho-CaMKII following TAC in KO mice results from the upregulation and activation of CaMKIIγ. PKD, another regulator of HDAC phosphorylation, has previously been shown to play a critical role in cardiac hypertrophic signaling (28, 34, 35). PKD activation, assessed by Western blotting using phospho-PKD (Ser916 and Ser744/748) antibodies, was increased by TAC in both WT and KO mice (Figure 3B). Thus the maintained hypertrophic response to TAC in mice with CaMKIIδ deletion could be explained by the upregulation of CaMKIIγ expression and/or PKD activation.

CaMKIIδ deletion inhibits the development of heart failure induced by long-term TAC. Our previous work demonstrated that TG mice with CaMKIIδ$_C$ overexpression developed severe heart failure (16). To further explore the role of endogenous CaMKIIδ in heart failure, an additional group of mice was subjected to TAC and assessed at both 2 and 6 weeks after TAC. Pressure gradients determined at 6 weeks after TAC were comparable in WT (88 ± 26 mmHg) and KO (87 ± 30 mmHg) mice. Cardiomyocyte cross-sectional area was increased to a similar extent in WT and KO mice 6 weeks after TAC (data not shown). Echocardiographic analysis revealed a comparable degree of hypertrophy in banded KO and WT mice, as indicated by interventricular septal thickness (IVS) and LV posterior wall thickness (LVPW), at both 2 and 6 weeks after TAC (Figure 4A).

Strikingly, however, whereas WT banded mice showed progressively increasing LV internal diameter (LVID) and decreasing fractional shortening (FS) at 2 and 6 weeks after TAC (Figure 4B), neither ventricular dilation nor systolic dysfunction significantly progressed in KO animals (Figure 4B). Increases in HW/BW and HW/TL ratios seen in WT mice after TAC were also greatly attenuated in the KO mice (Figure 5). Pulmonary congestion is a hallmark symptom of heart failure. In WT mice, 6-week TAC caused marked lung edema, manifested as an increase in relative lung weight (LW), and this response was markedly diminished in KO mice (Figure 5). Strikingly, KO mice subjected to TAC also showed improved survival compared with WT mice (Figure 4B), with 34% of WT mice dying within the first month after TAC compared with 12% lethality in KO mice.

Cardiac apoptosis and fibrosis both contribute to the phenotypic changes associated with heart failure. TUNEL staining was used to assess the number of apoptotic cells, and Masson-

Table 2
Hemodynamic analysis of the response to dobutamine in mice with CaMKIIδ deletion and their WT littermates

Parameter	Group	Dobutamine (μg/kg/min)					
		0	0.75	2	4	6	8
HR (bpm)	WT	384 ± 27	412 ± 33	442 ± 44	502 ± 58	577 ± 54	626 ± 48
HR (bpm)	KO	402 ± 50	425 ± 51	465 ± 52	527 ± 50	586 ± 60	626 ± 48
LVP (mmHg)	WT	135 ± 30	142 ± 34	152 ± 34	153 ± 29	154 ± 29	153 ± 25
LVP (mmHg)	KO	146 ± 12	154 ± 18	167 ± 20	170 ± 17	166 ± 25	159 ± 29
$+dP/dt_{max}$ (mmHg/s)	WT	10,093 ± 2,387	11,308 ± 2,856	13,907 ± 3,768	17,716 ± 3,357	20,637 ± 2,382	21,341 ± 2,290
$+dP/dt_{max}$ (mmHg/s)	KO	11,565 ± 1,136	12,280 ± 1,186	15,285 ± 1,944	18,777 ± 1,802	20,846 ± 1,950	20,965 ± 2,666
$-dP/dt_{max}$ (mmHg/s)	WT	–8,314 ± 1,594	–9,160 ± 1,784	–10,813 ± 2,289	–13,021 ± 2,455	–14,595 ± 2,276	–15,128 ± 2,013
$-dP/dt_{max}$ (mmHg/s)	KO	–9,559 ± 1,510	–10,392 ± 1,444	–12,443 ± 1,702	–14,321 ± 1,347	–15,567 ± 2,102	–15,220 ± 1,998
Exponential Tau (ms)	WT	11.04 ± 2.30	10.22 ± 2.00	9.18 ± 1.65	7.55 ± 1.42	6.70 ± 1.29	6.34 ± 1.10
Exponential Tau (ms)	KO	10.60 ± 1.36	10.84 ± 2.72	9.05 ± 1.05	7.66 ± 0.99	6.56 ± 0.73	6.31 ± 0.91

CaMKIIδ KO and WT mice at 3 months of age were subjected to hemodynamic detection. Data are expressed as mean ± SD of values from 8–9 mice. HR, heart rate; LVP, maximum end-systolic LV pressure; $+dP/dt_{max}$, maximum positive first derivative of LVP; $-dP/dt_{max}$, maximum negative first derivative of LVP.

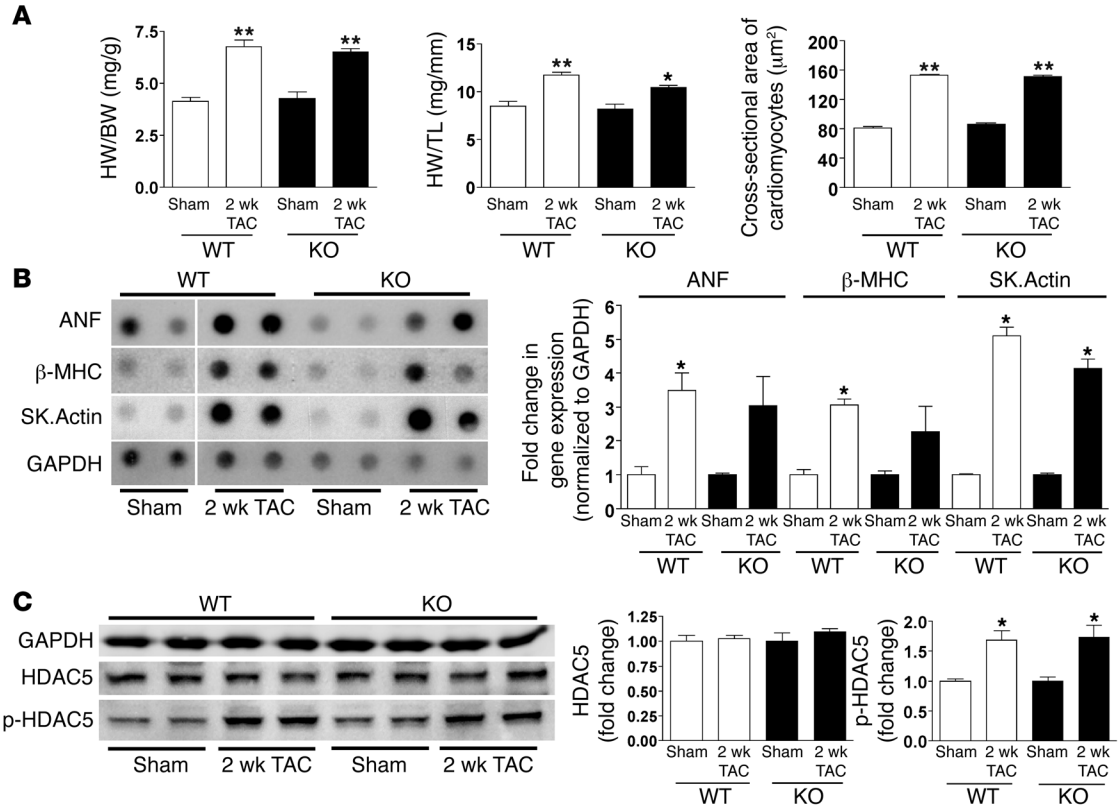

Figure 2

CaMKIIδ deletion does not prevent cardiac hypertrophy induced by 2-week TAC. (**A**) Relative HW, indicated by HW/BW or HW/TL ratios, and cross-sectional area of cardiomyocytes detected by wheat germ agglutinin staining. Data are mean ± SEM of values from 3–6 mice. (**B**) Hypertrophic gene expression in response to 2-week TAC. RNA isolated from ventricular tissue of WT and KO mice was subjected to dot blot analysis using gene transcript–specific antisense oligonucleotide probes. GAPDH was used as the normalizing control. Samples for WT sham were loaded on the same membrane as the other but were noncontiguous (denoted by white line). Sk.Actin, α-skeletal actin. Data are mean ± SEM of values from 3 determinations. (**C**) Expression and phosphorylation of HDAC5 (Ser498) in LV homogenates after 2-week TAC, as detected by Western blot analysis. Data are mean ± SEM of values from 3–4 determinations. *$P < 0.05$, **$P < 0.01$ versus sham.

trichrome staining was used to assess development of cardiac fibrosis, as indicated by interstitial collagen deposition. Both endpoints significantly increased after 6-week TAC in KO and WT hearts compared with sham-operated controls. Comparatively, however, both the number of TUNEL-positive cells and the extent of fibrosis induced by TAC were higher in WT than in KO mice (Figure 6, A and B). KO mice also showed less inflammatory cell recruitment after TAC, as evidenced by reduced myeloperoxidase activity (data not shown).

CaMKIIδ deletion normalizes the altered expression levels of Ca^{2+} regulatory proteins induced by long-term TAC. Abnormal intracellular Ca^{2+} homeostasis is an accepted pathogenic mechanism for heart failure and is associated with substantial alterations in the expression of Ca^{2+} regulatory proteins, including RyR2, sarcoplasmic or endoplasmic reticulum calcium ATPase2α (SERCA2α), and type 2 inositol 1,4,5 trisphosphate receptor (IP_3R2). Consistent with our previous studies and those of others (13, 17), decreased expression of RyR and SERCA2, and increased expression of IP_3R2, were observed in WT mice after 6-week TAC. These changes were largely ameliorated in KO mice (Figure 7). Of particular interest, after 6-week TAC, the IP_3R2/RyR ratio significantly increased (3.6-fold) in WT mice, but not in KO mice (Figure 7). Taken together, these results suggest that CaMKIIδ contributes to altered expression levels of Ca^{2+} regulatory proteins during the development of pressure overload–induced heart failure.

CaMKIIδ deletion reduces RyR2 phosphorylation during the development of heart failure induced by long-term TAC. The RyR2 has multiple phosphorylation sites, the best characterized of which are Ser2815 (Ser2814) phosphorylated by CaMKII, and Ser2809 (Ser2808) phosphorylated predominantly by PKA (36). An emerging body of evidence has demonstrated that aberrant RyR2 function caused by hyperphosphorylation at CaMKII or PKA site plays an important role in the development of heart failure (5, 16, 17, 37–40). Using phospho-specific antibodies, we determined that the fraction of total RyR2 phosphorylated at the CaMKII site (Ser2815) was significantly increased after 6-week TAC in WT mice but not in KO mice (Figure 7). Similar observations were made following 2-week TAC (data not shown), although the increase in RyR2 phosphorylation was less than that seen at 6 weeks after TAC. There was no significant increase in phosphorylation of RyR2 at the PKA site (Ser2809) in either WT or KO mice (Figure 7). These observations are consistent with the hypothesis that increased CaMKII-phosphorylated RyR2 contributes to the decompensation of pressure overload–induced heart failure.

CaMKIIδ deletion reduces Ca^{2+} leak during the development of heart failure induced by long-term TAC. We previously demonstrated that RyR2 phosphorylation by CaMKII enhanced diastolic Ca^{2+} leak

Table 3
LV dimension, wall thickness, and function in mice with CaMKIIδ deletion and their WT littermates in response to 2-week TAC

Parameter	WT 2-wk TAC		KO 2-wk TAC	
	Sham	TAC	Sham	TAC
IVSd (mm)	0.66 ± 0.03	0.81 ± 0.11[A]	0.66 ± 0.03	0.87 ± 0.15[A]
IVSs (mm)	1.19 ± 0.03	1.32 ± 0.15	1.13 ± 0.11	1.33 ± 0.21
LVPWd (mm)	0.62 ± 0.06	0.82 ± 0.14[A]	0.62 ± 0.02	0.88 ± 0.19[A]
LVPWs (mm)	1.12 ± 0.08	1.42 ± 0.20[A]	1.23 ± 0.13	1.38 ± 0.26
LVIDd (mm)	3.06 ± 0.19	3.53 ± 0.39	3.37 ± 0.16	3.50 ± 0.26
LVIDs(mm)	1.60 ± 0.08	1.98 ± 0.54	1.74 ± 0.28	2.12 ± 0.31
FS (%)	47.79 ± 1.51	44.47 ± 10.89	46.44 ± 6.15	41.20 ± 7.42

Data are expressed as mean ± SD of values from 3–6 mice. [A]$P < 0.05$ versus sham.

and suggested that this was causally related to the development of heart failure (17, 39). To assess SR Ca^{2+} leak as a functional correlate of RyR2 phosphorylation, we measured Ca^{2+} sparks in cardiomyocytes isolated from WT and KO mice (Figure 8) after sham surgery or 6-week TAC. There was no difference in baseline Ca^{2+} spark frequency (CaSpF) in sham-operated WT versus KO mice. Mean CaSpF tended to increase with TAC in WT (1.29 ± 0.44 versus 2.36 ± 0.77 spark/100 mm/s), but not in KO mice (1.34 ± 0.27 versus 0.47 ± 0.17 spark/100 mm/s). There was a highly significant difference in CaSpF in 6-week TAC cardiomyocytes from WT versus KO mice ($P < 0.01$; Figure 8). Thus CaMKIIδ deletion prevents enhancement of SR Ca^{2+} leak in this mouse model of pressure overload–induced heart failure. This is consistent with results in a rabbit pressure and volume overload heart failure model, in which CaMKII inhibition prevented increases in SR Ca^{2+} leak (13). The observed changes in SR Ca^{2+} leak are likely to result from alterations in RyR2 phosphorylation by CaMKIIδ, because SR Ca^{2+} content, as assessed by caffeine-induced Ca^{2+} transient, was not significantly different in any of the 4 groups.

Discussion

The current results provide multiple insights into the role of CaMKIIδ in the development of cardiac hypertrophy and heart failure. First, germline deletion of the predominant cardiac isoform of CaMKII had no major effect on basal cardiac structure or function. Second, activation of CaMKIIδ was not required for the development of cardiac hypertrophy in response to pressure overload. Third, CaMKIIδ was critically involved in cardiac decompensation after long-term pressure overload, because the absence of CaMKIIδ attenuated LV chamber dilation, cardiac dysfunction, pulmonary congestion, apoptosis, and fibrosis as well as improving survival. Finally, our findings further linked CaMKIIδ-mediated RyR2 phosphorylation to pressure overload–induced heart failure and SR Ca^{2+} leak. To our knowledge, our findings are the first to demonstrate a critical role for CaMKIIδ in development of heart failure independent of alterations in cardiac hypertrophy.

The role of CaMKIIδ in cardiac hypertrophy. We first reported that transient expression of $CaMKII\delta_B$ in neonatal rat ventricular myocytes results in transcriptional activation of an atrial natriuretic factor–luciferase (ANF-luciferase) reporter gene and enhanced ANF expression in response to phenylephrine (41). These data, along with our previous findings using CaMKII inhibitors (42), suggested a role for CaMKII in the initiation of cardiac hypertrophic growth. Subsequent work from our laboratory demonstrated that cardiac hypertrophy develops in transgenic mice that overexpress the $CaMKII\delta_B$ isoform in the heart (15, 18). Mice expressing $CaMKII\delta_C$ also initially demonstrate cardiac hypertrophy, but this rapidly transitions to a dilated cardiomyopathy with markedly decreased FS and premature death (16). A transcription factor, MEF2, identified as a downstream target for CaMK, is activated by CaMKII-mediated phosphorylation of HDACs and their dissociation from it (30, 43). Comparison of $CaMKII\delta_B$ and $CAMKII\delta_C$ mice at early stages indicates that both splice variants increase HDAC phosphorylation, mediate transcriptional MEF2 activation in vivo and in vitro, and induce

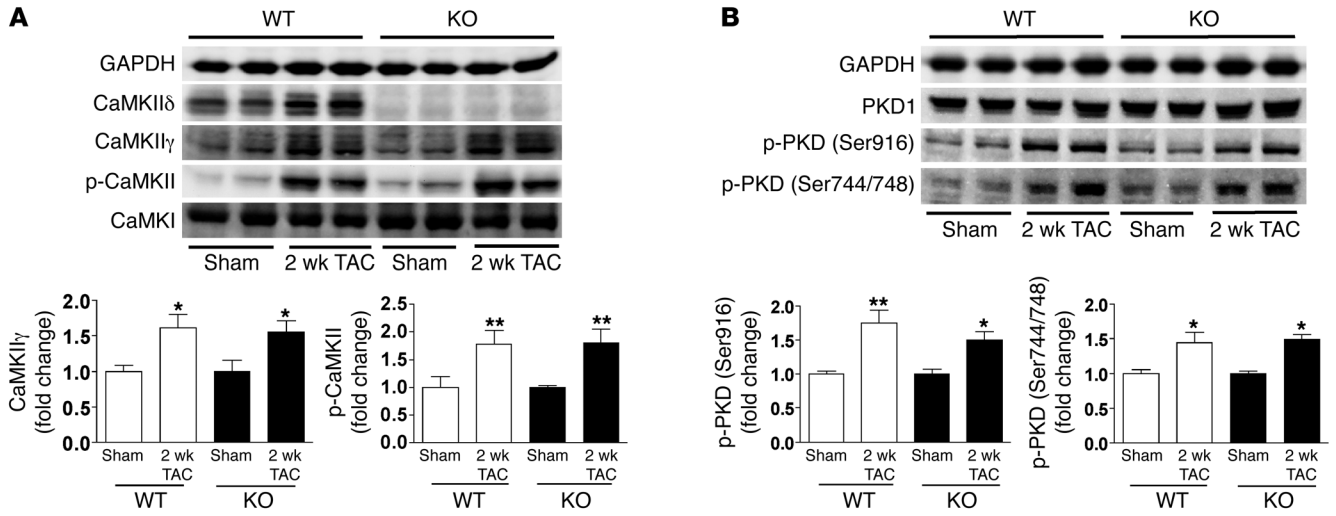

Figure 3
Upregulation of CaMKIIγ expression and PKD phosphorylation in cardiac hypertrophy. (**A**) Expression of CaMKIIδ, CaMKIIγ, CaMKI, and phospho-CaMKII in LV homogenates 2 weeks after TAC, as detected by Western blot analysis. (**B**) Expression of PKD1 and phospho-PKD (Ser916 and Ser744/748) in LV homogenates 2 weeks after TAC were detected by Western blot analysis. Data are mean ± SEM of values from 4–6 determinations. *$P < 0.05$, **$P < 0.01$ versus sham.

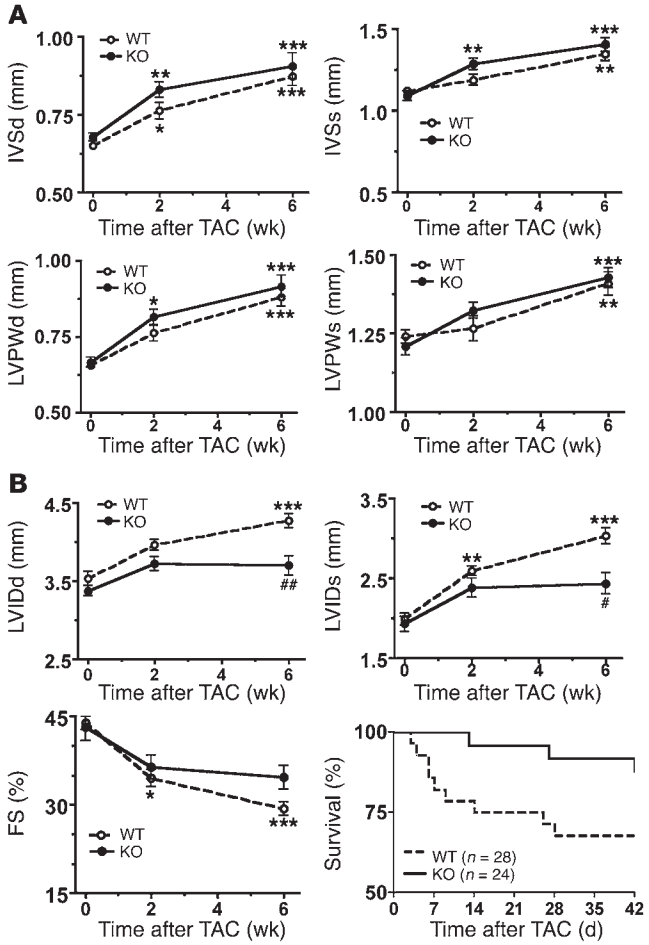

Figure 4
Effects of CaMKIIδ deletion on the development of cardiac hypertrophy and heart failure after 6-week TAC. Shown are averaged echocardiographic parameters and percent survival in WT and CaMKIIδ-deficient mice at different time points after TAC. Data are mean ± SEM of values from 12–18 mice, unless otherwise indicated. (**A**) Hypertrophic responses. (**B**) Decompensation to heart failure. Percent survival in response to TAC is plotted as a Kaplan-Meier curve ($P = 0.08$, WT versus KO). $^{*}P < 0.05$, $^{**}P < 0.01$, $^{***}P < 0.001$ versus pre-echocardiography; $^{\#}P < 0.05$, $^{\#\#}P < 0.01$ versus WT.

hypertrophic gene expression (18). This may explain why comparable cardiac hypertrophy is initially observed in CaMKIIδ$_B$ and CaMKIIδ$_C$ transgenic mice.

In light of the evidence implicating CaMKIIδ in cardiac gene expression and hypertrophy, we hypothesized that genetic deletion of CaMKIIδ would inhibit or decrease development of pathological hypertrophy. Remarkably, hypertrophy induced by pressure overload was comparable in KO and WT mice, as evidenced by gravimetric, echocardiographic, and cell size analysis. Consistent with this, we found similar increases in HDAC5 phosphorylation and hypertrophic gene expression in WT and KO mice 2 weeks after TAC. Thus while CaMKIIδ is activated in response to pressure overload and is able to induce hypertrophy when overexpressed, it is not required for the development of cardiac hypertrophy in response to TAC in our KO mouse model.

Alternative mechanisms for induction of cardiac hypertrophy. Another CaMKII isoform, CaMKIIγ, is present at low amounts in the heart, but has previously been shown to be upregulated by pressure overload (33). We demonstrated here that CaMKIIγ was also upregulated in mice in which CaMKIIδ was deleted. A CaMKIIγ variant cloned from brain contains a nuclear localization sequence and has previously been shown to distribute in nucleus as well as cytosol when expressed in NG108-15 cells (44). Our preliminary immunofluorescence studies indicate that CaMKIIγ was relatively concentrated in cardiac nuclei and that nuclear CaMKIIγ increased after TAC (data not shown). Accordingly, it is possible that CaMKIIγ, upregulated and activated after TAC, compensates for loss of CaMKIIδ in mediating HDAC phosphorylation and hypertrophic responses. Another member of the CaMK superfamily, PKD, has also been implicated in HDAC5 phosphorylation and export from the nucleus in response to hypertrophic stimuli (28). PKD is activated in pathophysiological hypertrophy and heart failure (14, 35), and, as shown here, it was activated to a similar extent in response to TAC in WT and KO mice. A recent study demonstrated that PKD1-null mice exhibit a diminished hypertrophic response to pressure overload or chronic adrenergic and angiotensin II signaling (34). Thus increased PKD might also serve to mediate hypertrophic responses to pressure overload in the absence of CaMKIIδ.

Further studies will be necessary to determine whether CaMKIIγ- or PKD-mediated mechanisms are responsible for the maintenance of TAC-induced hypertrophy in our KO mice. It is interesting, however, that increases in CaMKIIγ expression and PKD phosphorylation either do not occur or do not provide adequate compensation in another recently reported line of CaMKIIδ KO mice (27), perhaps as a result of differences in the age and background of the mice or duration and severity of TAC. Isoproterenol induced hypertrophy was also previously shown to be diminished in mice expressing AC3-I, a genetically encoded CaMKII inhibitor (19); however, we observed comparable hypertrophic responses to 9-day isoproterenol treatment in our WT and KO mice (data not shown). Fortuitously, the finding that hypertrophy was unaffected by CaMKIIδ deletion in our mouse model provided us the opportunity to assess the role of CaMKIIδ in decompensation to heart failure independent of potentially adaptive or maladaptive effects of an altered hypertrophic response.

The role of CaMKII in heart failure. Suggestive evidence for a causal role of CaMKII in the development of heart failure emerged from our prior observation that transgenic CaMKIIδ$_C$ expression in the myocardium leads to dilated cardiomyopathy and ventricular dysfunction (16). These findings, taken with abundant evidence for upregulated expression and activation of CaMKIIδ in humans and animal models of heart failure (11–14), provide support for a critical role for CaMKII in the pathogenesis of heart failure. Seminal studies from the Anderson laboratory demonstrated that inhibition of CaMKII with KN-93 or by transgenic expression of the CaMKII inhibitory peptide AC3-I prevented maladaptive remodeling induced by high levels of β-adrenergic receptor stimulation or by myocardial infarction (19). These studies did not, however, examine development of pressure overload–induced heart failure. In addition, since recent work indicates that AC3-I can inhibit multiple members of the CaMKII superfamily, including PKD (27), AC3-I might also block PKD-dependent pathophysiological remodeling (versus our CaMKIIδ-specific KO). To our knowledge, our current work is the first to demonstrate attenuated devel-

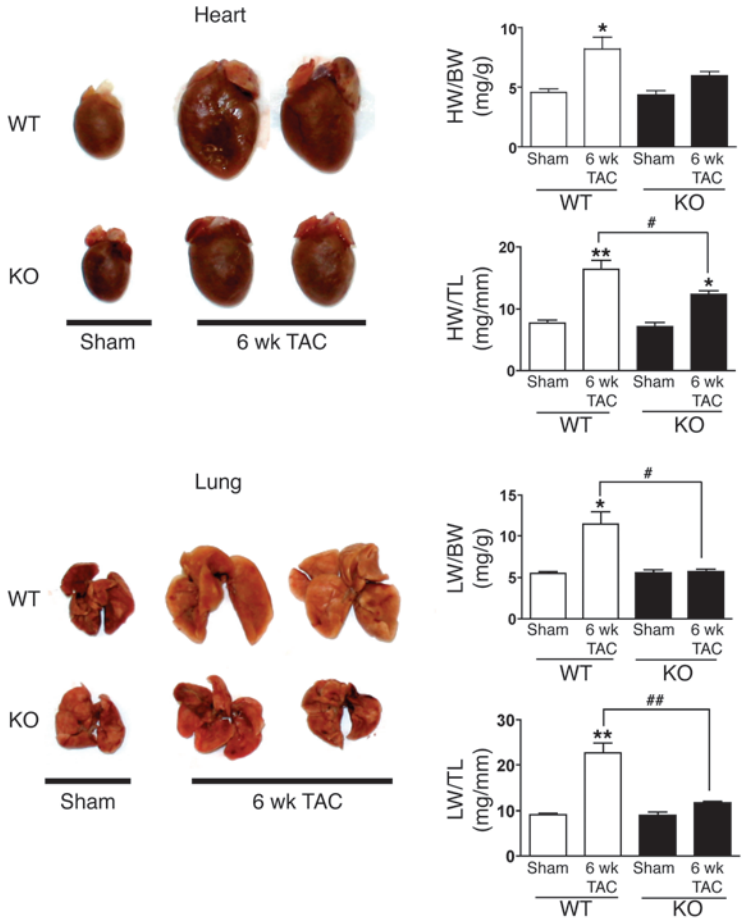

Figure 5
CaMKIIδ deletion reduces relative HW and lung edema in response to 6-week TAC. HW and LW were normalized to BW and TL. Data are mean ± SEM of values from 3–9 mice. $^{*}P < 0.05$, $^{**}P < 0.01$ versus sham; $^{\#}P < 0.05$, $^{\#\#}P < 0.01$ versus WT TAC.

opment of pressure overload–induced heart failure by selective CaMKIIδ ablation, which occurred without attenuation of the initial hypertrophic response. KO mice subjected to long-term TAC showed significantly reduced chamber dilation, ventricular dysfunction, lung edema, cardiac fibrosis, apoptosis, and death relative to WT mice. The observation that the salutary effects of CaMKIIδ deletion on the response to long-term pressure overload were seen in the absence of any diminution in the initial development of hypertrophy suggests that the benefit of CaMKIIδ deletion does not derive from inhibiting the expected progression of hypertrophy per se, but rather from involvement of CaMKIIδ in the decompensation to heart failure.

We hypothesize that CaMKIIγ or PKD can serve redundant functions with CaMKIIδ in supporting induction of cardiac hypertrophy. In contrast, CaMKIIγ or PKD do not compensate for loss of CaMKIIδ in regulating the transition to heart failure. This could reflect a predominant localization or signaling role for CaMKIIγ and PKD in the nucleus or limited access to or specificity for sarcoplasmic reticular targets involved in development of heart failure. This hypothesized specificity would be consistent with our previous observation that RyR2 and PLB phosphorylation is not increased in mice expressing the nuclear localized CaMKIIδ$_B$ (15, 18).

Decreases in the expression of SR regulatory proteins, including SERCA2 and RyR2, are prominent pathophysiological components of heart failure (13, 17). We found in the current study that both SERCA2 and RyR2 expression were significantly reduced in WT mice, but not KO mice, that were subjected to long-term pressure overload. Enhanced expression of IP_3R has also been observed in heart failure models (13, 45). We demonstrate here that IP_3R2 expression significantly increased in WT mice after TAC, but interestingly, this did not occur in KO mice. Further studies are required to determine whether the upregulated ventricular IP_3R2 contributes to arrhythmogenesis or to maladaptive transcriptional regulation. CaMKII can also phosphorylate the L-type Ca^{2+} channel or associated regulatory proteins, resulting in Ca^{2+} current (I_{Ca}) facilitation (7–10), or affect Na^+ channel gating (46) and the development of arrhythmia (47–50). Increased arrhythmogenesis is therefore a potential mechanism by which CaMKIIδ could contribute to lethality in heart failure and by which CaMKIIδ deletion might enhance survival following long-term TAC.

Cardiomyocyte apoptosis is now considered to be a hallmark and likely contributing mechanism in the transition from cardiac hypertrophy to heart failure. Several published papers demonstrate that CaMKII transduces signals leading to apoptosis in the heart (51–53). Indeed, β_1-adrenergic stimulation induces apoptosis in adult cardiomyocytes through CaMKII rather than PKA (51). In other studies, CaMKII inhibition (with either KN-93 or cardiac expression of the CaMKII inhibitor AC3-I) was shown to protect against apoptosis in ischemic insult (52, 53). Here we show that apoptosis and secondary cardiac fibrosis induced by long-term pressure overload were also significantly reduced in the absence of CaMKIIδ. Thus diminished CaMKIIδ and Ca^{2+}-dependent apoptosis may further contribute to the reduced heart failure phenotype seen in mice with CaMKIIδ deletion.

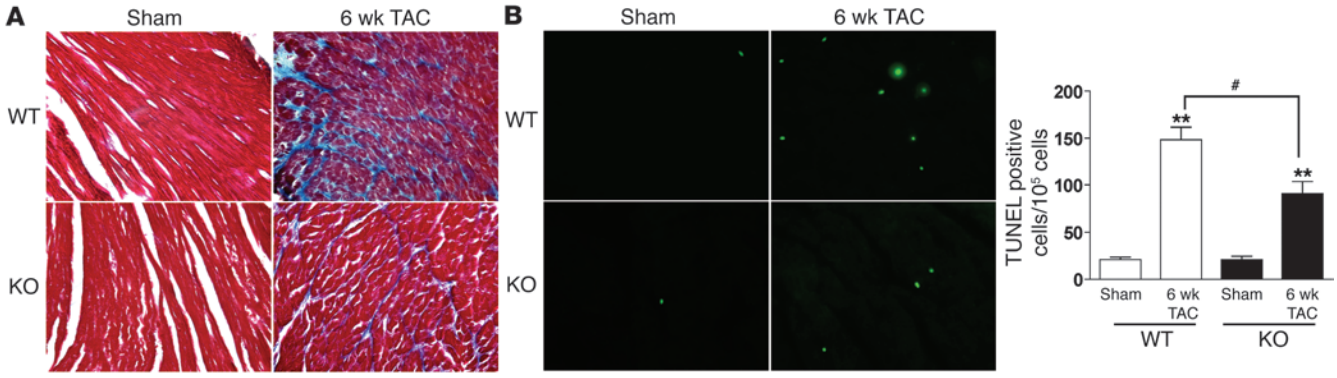

Figure 6
CaMKIIδ deletion inhibits cardiac fibrosis and apoptosis after 6-week TAC. (**A**) Interstitial collagen deposition, indicative of cardiac fibrosis, as assessed by Masson trichrome staining. (**B**) TUNEL staining of heart tissue after 6-week TAC in WT and KO mice. Original magnification, ×40. Data are mean ± SEM of values from 3 hearts per group, with at least 5,000 nuclei examined per heart. $^{**}P < 0.01$ versus sham; $^{\#}P < 0.05$ versus WT TAC.

Numerous lines of evidence indicate that altered RyR2 function contributes to cardiac dysfunction in heart failure. Our earlier studies in transgenic mice revealed that overexpression of CaMKIIδ$_C$ lead to RyR2 phosphorylation and increased diastolic SR Ca^{2+} leak. This preceded development of heart failure and was reversed by CaMKII inhibition (16, 17). The effect of CaMKII-dependent RyR2 phosphorylation is to enhance open channel probability (5, 6), SR Ca^{2+} leak (13, 17, 54), and fractional SR Ca^{2+} release during E-C coupling (55). Although there is controversy about the effect of RyR2 phosphorylation at its PKA versus CaMKII sites (13, 37, 54, 56, 57), there is uniform support for the notion that increased RyR2 sensitivity to Ca^{2+} and aberrant RyR2 function caused by hyperphosphorylation may be central mechanisms in the pathogenesis of heart failure (5, 16, 17, 37–39). We demonstrate here that the fraction of RyR2 phosphorylated at the CaMKII site increased during development of pressure overload–induced heart failure in WT mice, but not in KO mice. This was mirrored in our data measuring CaSpF, in which diastolic Ca^{2+} leak increased after 6-week TAC in WT but not KO mice. Accordingly, we suggest that the diminished RyR2 phosphorylation and SR Ca^{2+} leak seen in KO mice are protective mechanisms that limit decompensation to heart failure. We conclude that maintenance of normal RyR2 function underlies the beneficial role of CaMKIIδ deletion on progression to heart failure.

The list of molecules and signaling pathways implicated in the development of hypertrophy and heart failure continues to grow. Few molecules have been so broadly associated with heart failure, and so uniquely implicated in the functional regulation of Ca^{2+} handling proteins, as CaMKII. As a protein kinase, this enzyme has proven potential to be a therapeutic target. If, as our findings imply, CaMKII plays a more critical role in the transition to heart failure than in the development of hypertrophy, inhibition of CaMKII or its cytosolic targets may provide a means for selective blockade of these maladaptive changes.

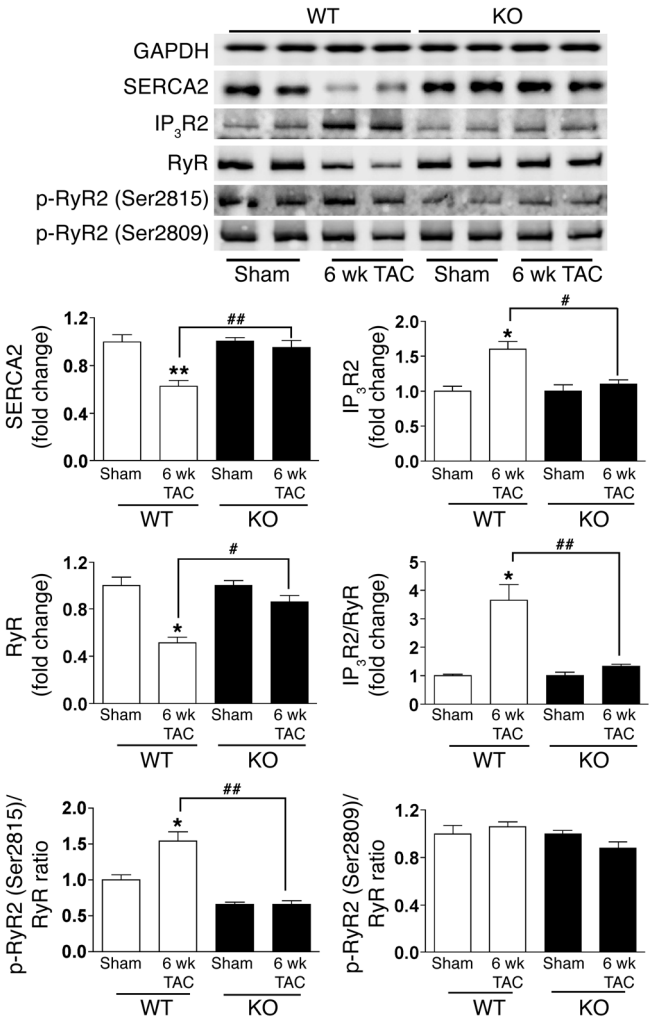

Figure 7
CaMKIIδ deletion normalizes the expression of Ca^{2+} regulatory proteins and reduces RyR2 phosphorylation at the CaMKII site after 6-week TAC. LV homogenates were subjected to Western blotting. Quantitative analysis is shown below. Phosphorylation of RyR2 at the CaMKII site (Ser2815) or at the PKA site (Ser2809) was normalized to RyR expression, and the IP$_3$R2/RyR ratio was also calculated. Data are mean ± SEM of 3–4 determinations. $^{*}P < 0.05$, $^{**}P < 0.01$ versus sham; $^{\#}P < 0.05$, $^{\#\#}P < 0.01$ versus WT TAC.

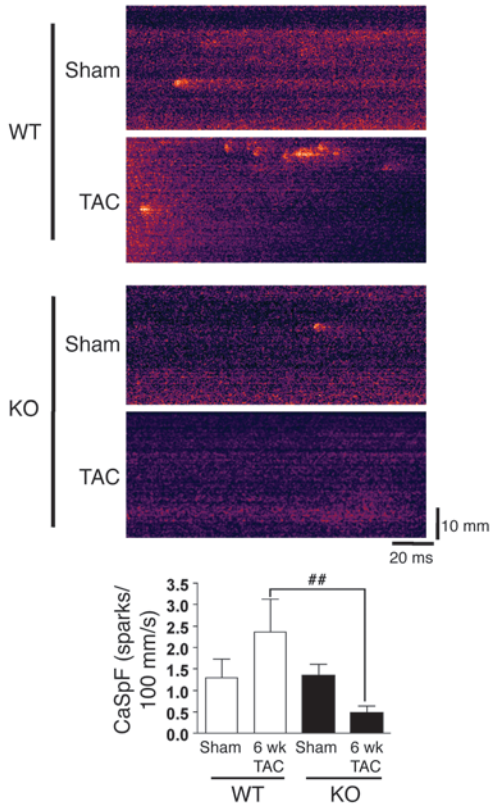

Figure 8
CaMKIIδ ablation reduces SR Ca^{2+} leak in 6-week TAC mice. Longitudinal line scan images of spontaneous Ca^{2+} sparks were recorded in myocytes from both genotypes with or without TAC. CaSpF data were averaged from isolated cardiomyocytes in WT sham (n = 10), WT 6-week TAC (n = 7), KO sham (n = 12), and KO 6-week TAC (n = 12) groups. $^{\#\#}P < 0.01$ versus WT TAC. There was no significant difference between KO and WT 6-week TAC mice with respect to SR Ca^{2+} content, assessed by caffeine-induced Ca^{2+} transient amplitude (fluorescence normalized to baseline, WT, 4.2 ± 0.5; KO, 3.8 ± 0.8).

Methods

Gene targeting and generation of mice with CaMKIIδ deletion. The *Camk2d* genomic DNA was isolated from a 129SVJ mouse genomic library and used to construct the *Camk2d* targeting vector by standard techniques (58). Briefly, the *Camk2d* gene was cloned into a targeting vector that contained a neomycin selection cassette flanked by Flp recombinase target sites. Exons 9–11 of the *Camk2d* catalytic domain were inserted into 2 flanking LoxP sites (Figure 1A). The targeting construct was verified by sequencing and linearized with NotI before electroporation into ES cells at the UCSD Transgenic Core Facility. G418-resistant ES clones were screened for homologous recombination by Southern blotting. We microinjected 2 targeted clones into C57BL/B6 blastocysts, which were transferred into pseudopregnant mice to generate male chimeras. Male chimeras were bred with female Black Swiss mice to generate germline transmitted floxed heterozygous mice. These mice were subsequently crossed with protamine-Cre (Pro-Cre) mice (59) to generate mice that were doubly heterozygous for the *Camk2d* floxed allele and the Pro-Cre allele. The male mice were next crossed to female breeders in order to generate germline heterozygous null mutant offspring. Homozygous null mutant mice were generated by intercrosses of the heterozygous mice and were genotyped by PCR analysis using mouse tail DNA and specific primers for the WT (forward, 5′-GGAGCATTTCATCTGTAGGTG-3′; reverse, 5′-CAGATGTGCCTGACCAATATG-3′) and mutant (neo-specific primer: forward, 5′-AATGGGCTGACCGCTTCCTCGT-3′; reverse, 5′-CGATCATCAAGCTGAACAGCTGC-3′) alleles. The genotyping was confirmed by Southern blotting with *Eco*RI-digested genomic DNA and a ^{32}P-labeled probe. The WT allele was represented by a 13.4-kb band, whereas the 3.9-kb band represented the mutant allele. All procedures were performed in accordance with the NIH *Guide for the Care and Use of Laboratory Animals* and approved by the Institutional Animal Care and Use Committee of UCSD.

Echocardiographic and hemodynamic measurements. LV wall thickness, chamber dimension, and contractility were evaluated by noninvasive transthoracic echocardiography, as described previously (16). The following parameters were measured digitally: heart rate, LVID in diastole and in systole (LVIDd and LVIDs, respectively), and LVPWd and LVPWs. LV FS was calculated as (LVIDd − LVIDs)/LVIDd and expressed as a percentage. For hemodynamic analysis, mice were subjected to i.v. stimulation with dobutamine, a β-adrenergic agonist, and cardiac performance was detected as described previously (15). The following parameters were averaged from 12 beats: heart rate; maximum end-systolic LV pressure (LVP); maximum positive and negative first derivative of LVP; and exponential Tau, using a linear regression fit of the relation between dP/dt and pressure during isovolumic pressure decline.

TAC surgery and gravimetric analysis. TAC was performed on 8- to 12-week-old male KO and WT mice as described previously (16), with minor changes. Sham-operated mice were subjected to identical interventions except for the constriction of the aorta. After echocardiographic analysis at different time points, mice were anesthetized with ketamine/xylazine, and pressure gradients were measured to ensure similar pressure overload in WT and KO groups. KO and WT mice were sacrificed by cervical dislocation, and hearts and lungs were removed and weighed promptly. Relative HW and LW were calculated as HW/BW, LW/BW, HW/TL, or LW/TL ratios.

Heart tissue preparation. The LVs were transversely dissected. Part of the LV was frozen quickly in liquid nitrogen for protein and RNA analysis. The other part was fixed for 24 hours in 4% paraformaldehyde dissolved in 0.1 M PBS (pH 7.4), subsequently embedded in paraffin, and transversely cut into 5-μm sections for further histological analysis.

Protein and RNA analysis. Proteins from heart tissue were isolated, and Western blot analysis was performed according protocols described previously (15). The antibodies for immunoblotting were as follows: CaMKIIδ, CaMKIIγ, PLB, CaMKI, and α-actinin (Santa Cruz); PKD, phospho-PKD (Ser916 and Ser744/748), and GAPDH (Cell Signaling); phospho-PLB at CaMKII site (Thr17) and PKA site (Ser16) (Badrilla); RyR and phospho-CaMKII (Affinity Bioreagents); phospho-RyR2 at CaMKII site (Ser2815) and PKA site (Ser2809) (obtained from A.R. Marks, Columbia University, New York, New York, USA); and HDAC5 and phospho-HDAC5 (Ser498) (Assay Biotech). Total RNA was prepared from ventricular tissue using TRIzol reagent (Gibco, Invitrogen), and expression of fetal cardiac genes was determined by dot blot analysis of total ventricular RNA using ^{32}P-labeled oligonucleotide probes as described previously (15).

Histomorphometry and TUNEL assay. Paraffin sections were deparaffinized and subsequently subjected to FITC-labeled wheat germ agglutinin (Sigma-Aldrich) staining of membranes. To obtain cardiomyocyte short axis cross-sectional area in the LV, an average of 200–500 cardiomyocytes per animal was analyzed with Image J (http://rsbweb.nih.gov/ij/). The collagen deposition indicative of myocardial interstitial fibrosis was determined from Masson trichrome–stained sections. In situ DNA fragmentation was

assessed using TUNEL assay, and the number of TUNEL-positive cells was determined in 3 sections per group.

Ca^{2+} spark record. Ca^{2+} sparks were recorded in isolated mouse ventricular myocytes loaded with the Ca^{2+} indicator Fluo-3 AM, as previously described (60). Line scan images were obtained on a confocal microscope (Pascal, ×63 objective; Zeiss) with argon laser excitation (488 nm) every 1.5 ms (emission, >505 nm). Spontaneous Ca^{2+} sparks were recorded, after steady-state 1-Hz stimulation, in normal Tyrode solution (140 mM NaCl, 4 mM KCl, 1.1 mM $MgCl_2$, 10 mM HEPES, 10 mM glucose, 1.8 mM $CaCl_2$; pH 7.4) with NaOH. Caffeine (10 mM) was applied rapidly to assess SR Ca^{2+} content. Image analyses used homemade routines in interactive data language.

Statistics. Data are presented as mean ± SEM or mean ± SD as indicated and were analyzed by 2-tailed Student's *t* test between 2 groups or by ANOVA when 3 or more groups were compared. A *P* value less than 0.05 was considered statistically significant.

Acknowledgments

This work was supported by NIH grant P01 HL080101. H. Ling is supported by an American Heart Association Post-Doctoral Fellowship.

Received for publication November 11, 2008, and accepted in revised form February 25, 2009.

Address correspondence to: Joan Heller Brown, Department of Pharmacology, University of California, San Diego, 9500 Gilman Drive, La Jolla, California 92093-0636, USA. Phone: (858) 822-5858; Fax: (858) 822-4011; E-mail: jhbrown@ucsd.edu.

1. Bassani, R.A., Mattiazzi, A., and Bers, D.M. 1995. CaMKII is responsible for activity-dependent acceleration of relaxation in rat ventricular myocytes. *Am. J. Physiol.* **268**:H703–H712.
2. Hain, J., Onoue, H., Mayrleitner, M., Fleischer, S., and Schindler, H. 1995. Phosphorylation modulates the function of the calcium release channel of sarcoplasmic reticulum from cardiac muscle. *J. Biol. Chem.* **270**:2074–2081.
3. Karczewski, P., Kuschel, M., Baltas, L.G., Bartel, S., and Krause, E.G. 1997. Site-specific phosphorylation of a phospholamban peptide by cyclic nucleotide- and Ca^{2+}/calmodulin-dependent protein kinases of cardiac sarcoplasmic reticulum. *Basic Res. Cardiol.* **92**(Suppl. 1):37–43.
4. Witcher, D.R., Kovacs, R.J., Schulman, H., Cefali, D.C., and Jones, L.R. 1991. Unique phosphorylation site on the cardiac ryanodine receptor regulates calcium channel activity. *J. Biol. Chem.* **266**:11144–11152.
5. Wehrens, X.H., Lehnart, S.E., Reiken, S.R., and Marks, A.R. 2004. Ca^{2+}Calmodulin-dependent protein kinase ii phosphorylation regulates the cardiac ryanodine receptor. *Circ. Res.* **94**:E61–E70.
6. Maier, L.S., and Bers, D.M. 2002. Calcium, calmodulin, and calcium-calmodulin kinase II: heartbeat to heartbeat and beyond. *J. Mol. Cell. Cardiol.* **34**:919–939.
7. Anderson, M.E., Braun, A.P., Schulman, H., and Premack, B.A. 1994. Multifunctional Ca^{2+}/calmodulin-dependent protein kinase mediates Ca^{2+}-induced enhancement of the L-type Ca^{2+} current in rabbit ventricular myocytes. *Circ. Res.* **75**:854–861.
8. Dzhura, I., Wu, Y., Colbran, R.J., Balser, J.R., and Anderson, M.E. 2000. Calmodulin kinase determines calcium-dependent facilitation of L-type calcium channels. *Nat. Cell Biol.* **2**:173–177.
9. Xiao, R.-P., Cheng, H., Lederer, W.J., Suzuki, T., and Lakatta, E.G. 1994. Dual regulation of Ca^{2+}/calmodulin-dependent kinase II activity by membrane voltage and by calcium influx. *Proc. Natl. Acad. Sci. U. S. A.* **91**:9659–9663.
10. Yuan, W., and Bers, D.M. 1994. Ca^{2+}-dependent facilitation of cardiac Ca^{2+} current is due to Ca^{2+}-calmodulin-dependent protein kinase. *Am. J. Physiol.* **267**:H982–H993.
11. Hoch, B., Meyer, R., Hetzer, R., Krause, E.-G., and Karczewski, P. 1999. Identification and expression of d-isoforms of the multifunctional Ca^{2+}/calmodulin dependent protein kinase in failing and nonfailing human myocardium. *Circ. Res.* **84**:713–721.
12. Kirchhefer, U., Schmitz, W., Scholz, H., and Neumann, J. 1999. Acitivity of cAMP-dependent protein kinase and Ca^{2+}/calmodulin-dependent protein kinase in failing and nonfailing human hearts. *Cardiovasc. Res.* **42**:254–261.
13. Ai, X., Curran, J.W., Shannon, T.R., Bers, D.M., and Pogwizd, S.M. 2005. Ca^{2+}/calmodulin-dependent protein kinase modulates cardiac ryanodine receptor phosphorylation and sarcoplasmic reticulum Ca^{2+} leak in heart failure. *Circ. Res.* **97**:1314–1322.
14. Bossuyt, J., et al. 2008. Ca^{2+}/calmodulin-dependent protein kinase IIdelta and protein kinase D overexpression reinforce the histone deacetylase 5 redistribution in heart failure. *Circ. Res.* **102**:695–702.
15. Zhang, T., et al. 2002. The cardiac-specific nuclear d_B isoform of Ca^{2+}/calmodulin-dependent protein kinase II induces hypertrophy and dilated cardiomyopathy associated with increased protein phosphatase 2A activity. *J. Biol. Chem.* **277**:1261–1267.
16. Zhang, T., et al. 2003. The d_C isoform of CaMKII is activated in cardiac hypertrophy and induces dilated cardiomyopathy and heart failure. *Circ. Res.* **92**:912–919.
17. Maier, L.S., Zhang, T., Chen, L., DeSantiago, J., Brown, J.H., and Bers, D.M. 2003. Transgenic $CaMKIId_C$ overexpression uniquely alters cardiac myocyte Ca^{2+} handling: reduced SR Ca^{2+} load and activated SR Ca^{2+} release. *Circ. Res.* **92**:904–911.
18. Zhang, T., et al. 2007. CaMKIIdelta isoforms differentially affect calcium handling but similarly regulate HDAC/MEF2 transcriptional responses. *J. Biol. Chem.* **282**:35078–35087.
19. Zhang, R., et al. 2005. Calmodulin kinase II inhibition protects against structural heart disease. *Nat. Med.* **11**:409–417.
20. Wu, Y., et al. 2006. Suppression of dynamic Ca(2+) transient responses to pacing in ventricular myocytes from mice with genetic calmodulin kinase II inhibition. *J. Mol. Cell Cardiol.* **40**:213–223.
21. Li, J., et al. 2006. Calmodulin kinase II inhibition shortens action potential duration by upregulation of K^+ currents. *Circ. Res.* **99**:1092–1099.
22. Tobimatsu, T., and Fujisawa, H. 1989. Tissue specific expression of four types of rat calmodulin-dependent protein kinase II transcripts. *J. Biol. Chem.* **264**:17907–17912.
23. Edman, C.F., and Schulman, H. 1994. Identification and characterization of delta B-CaM kinase and delta C-CaM kinase from rat heart, two new multifunctional Ca^{2+}/calmodulin-dependent protein kinase isoforms. *Biochim. Biophys. Acta.* **1221**:89–101.
24. Mayer, P., Möhlig, M., Idlibe, D., and Pfeiffer, A. 1995. Novel and uncommon isoforms of the calcium sensing enzyme calcium/calmodulin dependent protein kinase II in heart tissue. *Basic Res. Cardiol.* **90**:372–379.
25. Baltas, L.G., Karczewski, P., and Krause, E.-G. 1995. The cardiac sarcoplasmic reticulum phospholamban kinase is a distinct d-CaM kinase isozyme. *FEBS Lett.* **373**:71–75.
26. Schworer, C.M., Rothblum, L.I., Thekkumkara, T.J., and Singer, H.A. 1993. Identification of novel isoforms of the d subunit of Ca^{2+}/calmodulin-dependent protein kinase II. *J. Biol. Chem.* **268**:14443–14449.
27. Backs, J., et al. 2009. The {delta} isoform of CaM kinase II is required for pathological cardiac hypertrophy and remodeling after pressure overload. *Proc. Natl. Acad. Sci. U. S. A.* **106**:2342–2347.
28. Vega, R.B., et al. 2004. Protein kinases C and D mediate agonist-dependent cardiac hypertrophy through nuclear export of histone deacetylase 5. *Mol. Cell. Biol.* **24**:8374–8385.
29. Wu, X., et al. 2006. Local InsP3-dependent perinuclear Ca^{2+}signaling in cardiac myocyte excitation-transcription coupling. *J. Clin. Invest.* **116**:675–682.
30. Backs, J., Song, K., Bezprozvannaya, S., Chang, S., and Olson, E.N. 2006. CaM kinase II selectively signals to histone deacetylase 4 during cardiomyocyte hypertrophy. *J. Clin. Invest.* **116**:1853–1864.
31. Singer, H.A., Benscoter, H.A., and Schworer, C.M. 1997. Novel Ca^{2+}/calmodulin-dependent protein kinase II g-subunit variants expressed in vascular smooth muscle, brain, and cardiomyocytes. *J. Biol. Chem.* **272**:9393–9400.
32. Bayer, K.U., Lohler, J., Schulman, H., and Harbers, K. 1999. Developmental expression of the CaM kinase II isoforms: ubiquitous gamma- and delta-CaM kinase II are the early isoforms and most abundant in the developing nervous system. *Brain Res. Mol. Brain Res.* **70**:147–154.
33. Colomer, J.M., Mao, L., Rockman, H.A., and Means, A.R. 2003. Pressure overload selectively up-regulates Ca2+/calmodulin-dependent protein kinase II in vivo. *Mol. Endocrinol.* **17**:183–192.
34. Fielitz, J., et al. 2008. Requirement of protein kinase D1 for pathological cardiac remodeling. *Proc. Natl. Acad. Sci. U. S. A.* **105**:3059–3063.
35. Harrison, B.C., et al. 2006. Regulation of cardiac stress signaling by protein kinase d1. *Mol. Cell Biol.* **26**:3875–3888.
36. Huke, S., and Bers, D.M. 2008. Ryanodine receptor phosphorylation at Serine 2030, 2808 and 2814 in rat cardiomyocytes. *Biochem. Biophys. Res. Commun.* **376**:80–85.
37. Marx, S.O., et al. 2000. PKA phosphorylation dissociates FKBP12.6 from the calcium release channel (ryanodine receptor): defective regulation in failing hearts. *Cell.* **101**:365–376.
38. Wehrens, X.H., et al. 2006. Ryanodine receptor/calcium release channel PKA phosphorylation: a critical mediator of heart failure progression. *Proc. Natl. Acad. Sci. U. S. A.* **103**:511–518.
39. Kohlhaas, M., et al. 2006. Increased sarcoplasmic reticulum calcium leak but unaltered contractility by acute CaMKII overexpression in isolated rabbit cardiac myocytes. *Circ. Res.* **98**:235–244.
40. Marks, A.R. 2001. Ryanodine receptors/calcium release channels in heart failure and sudden cardiac death. *J. Mol. Cell. Cardiol.* **33**:615–624.
41. Ramirez, M.T., Zhao, X., Schulman, H., and Brown, J.H. 1997. The nuclear d_B isoform of Ca^{2+}/calmodulin-dependent protein kinase II regulates atrial natriuretic factor gene expression in ventricular myocytes. *J. Biol. Chem.* **272**:31203–31208.

42. Sei, C.A., et al. 1991. a-Adrenergic stimulation of atrial natriuretic factor expression in cardiac myocytes requires calcium influx, protein kinase C and calmodulin-regulated pathways. *J. Biol. Chem.* **266**:15910–15916.
43. Passier, R., et al. 2000. CaM kinase signaling induces cardiac hypertrophy and activates the MEF2 transcription factor in vivo. *J. Clin. Invest.* **105**:1395–1406.
44. Takeuchi, Y., Fukunaga, K., and Miyamoto, E. 2002. Activation of nuclear Ca(2+)/calmodulin-dependent protein kinase II and brain-derived neurotrophic factor gene expression by stimulation of dopamine D2 receptor in transfected NG108-15 cells. *J. Neurochem.* **82**:316–328.
45. Go, L.O., et al. 1995. Differential regulation of two types of intracellular calcium release channels during end-stage heart failure. *J. Clin. Invest.* **95**:888–894.
46. Wagner, S., et al. 2006. Ca^{2+}/calmodulin-dependent protein kinase II regulates cardiac Na^{+} channels. *J. Clin. Invest.* **116**:3127–3138.
47. Anderson, M.E., et al. 1998. KN-93, an inhibitor of multifunctional Ca^{2+}/calmodulin-dependent protein kinase, decreases early afterdepolarizations in rabbit heart. *J. Pharmacol. Exp. Ther.* **287**:996–1006.
48. Wu, Y., Roden, D.M., and Anderson, M.E. 1999. Calmodulin kinase inhibition prevents development of the arrhythmogenic transient inward current. *Circ. Res.* **84**:906–912.
49. Wu, Y., MacMillan, L.B., McNeill, R.B., Colbran, R.J., and Anderson, M.E. 1999. CaM kinase augments cardiac L-type Ca^{2+} current: a cellular mechanism for long Q-T arrhythmias. *Am. J. Physiol.* **276**:H2168–H2178.
50. Wu, Y., et al. 2002. Calmodulin kinase II and arrhythmias in a mouse model of cardiac hypertrophy. *Circulation.* **106**:1288–1293.
51. Zhu, W.Z., et al. 2003. Linkage of b_1-adrenergic stimulation to apoptotic heart cell death through protein kinase A-independent activation of Ca^{2+}/calmodulin kinase II. *J. Clin. Invest.* **111**:617–625.
52. Yang, Y., et al. 2006. Calmodulin kinase II inhibition protects against myocardial cell apoptosis in vivo. *Am. J. Physiol Heart Circ. Physiol.* **291**:H3065–H3075.
53. Vila-Petroff, M., et al. 2007. CaMKII inhibition protects against necrosis and apoptosis in irreversible ischemia-reperfusion injury. *Cardiovasc. Res.* **73**:689–698.
54. Guo, T., Zhang, T., Mestril, R., and Bers, D.M. 2006. Ca^{2+}/Calmodulin-dependent protein kinase II phosphorylation of ryanodine receptor does affect calcium sparks in mouse ventricular myocytes. *Circ. Res.* **99**:398–406.
55. Li, L., Satoh, H., Ginsburg, K.S., and Bers, D.M. 1997. The effect of Ca^{2+}-calmodulin-dependent protein kinase II on cardiac excitation-contraction coupling in ferret ventricular myocytes. *J. Physiol.* **501**:17–31.
56. Reiken, S., et al. 2003. Protein kinase A phosphorylation of the cardiac calcium release channel (ryanodine receptor) in normal and failing hearts. Role of phosphatases and response to isoproterenol. *J. Biol. Chem.* **278**:444–453.
57. Rodriguez, P., Bhogal, M.S., and Colyer, J. 2003. Stoichiometric phosphorylation of cardiac ryanodine receptor on serine-2809 by calmodulin-dependent kinase II and protein kinase A. *J. Biol. Chem.* **278**:38593–38600.
58. Zhou, Q., et al. 2001. Ablation of Cypher, a PDZ-LIM domain Z-line protein, causes a severe form of congenital myopathy. *J. Cell Biol.* **155**:605–612.
59. O'Gorman, S., Dagenais, N.A., Qian, M., and Marchuk, Y. 1997. Protamine-Cre recombinase transgenes efficiently recombine target sequences in the male germ line of mice, but not in embryonic stem cells. *Proc. Natl. Acad. Sci. U. S. A.* **94**:14602–14607.
60. Pereira, L., et al. 2007. The cAMP binding protein Epac modulates Ca^{2+}sparks by a Ca^{2+}/calmodulin kinase signalling pathway in rat cardiac myocytes. *J. Physiol.* **583**:685–694.